Trace of the Thermally Induced Evolution Mechanism of Interactions Between Water and Ionic Liquids

ARTICLE *in* THE JOURNAL OF PHYSICAL CHEMISTRY B · JULY 2010

Impact Factor: 3.3 · DOI: 10.1021/jp1041525 · Source: PubMed

2 AUTHORS:

Bingjie Sun
Fudan University
12 PUBLICATIONS **362** CITATIONS
SEE PROFILE

Peiyi wu
Fudan University
218 PUBLICATIONS **3,620** CITATIONS
SEE PROFILE

Trace of the Thermally Induced Evolution Mechanism of Interactions Between Water and Ionic Liquids

Bingjie Sun and Peiyi Wu*

The Key Laboratory of Molecular Engineering of Polymers (Ministry of Education) and Department of Macromolecular Science and Advanced Materials Laboratory, Fudan University, Shanghai 200433, PR China

Received: May 7, 2010; Revised Manuscript Received: June 14, 2010

The thermally induced evolution mechanisms of various interactions in ionic liquids (1-butyl-3-methylimidazolium tetrafluoroborate, bmimBF_4) and water mixtures have been investigated in this paper. In the near-infrared (NIR) spectroscopy, we focus mainly on ν(OH) and ν(CH) overtone regions. During heating of bmimBF_4 and water mixtures, the ν(OH) overtone peak shows a significant blue shift, and the area of this peak shows different changes in three heating regions. By using the perturbation correlation moving window (PCMW) method, we have ascertained the critical temperatures of these three regions: 25−100, 105−160, and 165−190 °C, and we have accordingly performed 2D correlation NIR analysis in three parts. On the basis of 2D study results, we find several types of O−H involved hydrogen bonds (H-B's) in a bmimBF_4 and water (15 mol %) mixture and arrive at their evolution mechanisms in each heating region. During heating at 25−100 °C, strong H-B's, such as BF_4^-···water···BF_4^- and BF_4^-···cyclic water dimer···BF_4^-, transform into weaker H-B's with simpler structures; at 105−160 °C, the remaining BF_4^-···water···BF_4^- continues to dissociate, and cation···water H-B's start to dissociate, and a large amount of released free water evaporates; whereas in the final heating region of 165−190 °C, BF_4^-···water···BF_4^- still exists and continues to dissociate, and in the study of the ν(CH) overtone region, we have found that the concentration of water in bmimBF_4 affects interactions between cations and anions. In the mixture of bmimBF_4 with more water (15 mol %), H-B's between water and bmimBF_4 cannot be completely destroyed, even at very high temperature; therefore, only limited new electrostatic interactions would be formed between cations and anions during heating, but in a mixture of bmimBF_4 with less water (15 mol %), cations and anions are able to form new electrostatic interactions during the heating process. However, the intensity of these interactions is smaller than that in the 80 °C isothermal process due to the low contacting possibilities among ions at high temperatures.

1. Introduction

Ionic liquids (ILs) are organic salts that are composed of asymmetric cations and anions, and they exist in the molten state at room temperature.[1−3] The general chemical structure of ionic liquids is shown in Figure 1. Various cations and anions can be matched to produce expected properties; therefore, ILs are also called "designer compounds".[4−9] ILs have numerous advantages, such as negligible vapor pressures, high thermal stability, superiority in electrochemistry, and environmentally friendly properties.[4,10−14] On the basis of these merits, increasing interest has been focused on ILs, and many applications have been performed with ILs, such as using them in lithium ion batteries,[10,15,16] capacitors,[17−19] and fuel cell electrolytes.[20]

Recently, solvents have also been mixed with ILs to optimize the properties of the ILs and expand the applications.[21,22] Among various solvents, water is a widely used type because water might affect properties of ILs in many aspects, such as density,[23−26] surface tension,[23,24] viscosity,[25,27] heat capacity,[28] electrical conductivity,[29] and solubility.[30−32]

Voth et al. found a micelle-like structure existing in dry ionic liquids by the molecular dynamics simulation method.[33,34] The micelle-like structure will be influenced by the addition of water, and this structure is maintained when the water content is 75−80 mol %, but collapses when the water content is up to 91−95 mol %.[34,35] This effect is caused by the hydrogen bonds (H-B's) formed between water molecules and the ions of the ILs.[36,37] Further research has shown that both cations and anions of ionic liquids can interact with water through H-B's.[36−38] Up to now, a number of studies have been performed on such H-B's interactions,[38−40] among which the FTIR spectroscopy method has been quite powerful because it is highly sensitive to changes of molecular circumstances.[36,41−43]

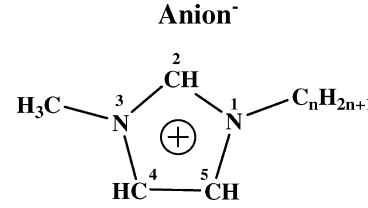

Figure 1. General chemical structure; *n* refers to the number of carbon atoms on the alkyl chain.

Lendl has used IR and 2DIR (two-dimensional infrared spectroscopy) methods and discovered H-B's between water and BF_4^- of ionic liquids could exist in three formations: BF_4^-···water, BF_4^-···water···BF_4^-, and BF_4^-···cyclic water dimer···BF_4^-.[38] In our previous work,[44] we have also confirmed the existence of these H-B's and concluded the dynamic mechanism of interactions between water and bmimBF_4 during isothermal conditions at 80 °C, finding that due to the evaporation of water, H-B's between water and anions or water and

* Corresponding author. Fax: +86-21-65640293. E-mail: peiyiwu@fudan.edu.cn.

10.1021/jp1041525
Published on Web 06/25/2010

cations are gradually destroyed, and after that, the released free cations and anions will interact with each other and form new electrostatic interactions.

On the basis of previous studies, we observe that the 2D correlation technique can greatly improve the power of spectroscopic investigations.[45−47] This method enables the study of spectral intensity fluctuations under an external perturbation such as temperature, time, pH, or concentration, etc.[48−54] Specific dynamic sequences of various chemical structures can be concluded by this method. In addition, 2D spectra can greatly improve the spectral resolution, such as separating overlapped peaks in the 1D spectra and discerning the exact positions of peaks. As a supplement of 2DIR, the newly developed perturbation correlation moving window (PCMW) technique is also very useful.[55] This method introduces the perturbation variable into the correlation equation; thus, it enables accurate capture of critical transition points of complicated spectral variations.

However, previous FTIR studies still have certain limitations. For example, most studies have focused on the MIR (mid-infrared) region, whereas less attention has been paid to NIR (near-infrared) spectroscopy study, which is supposed to enable us to obtain more useful information. As we know, strong H-B's show more significant absorption peaks in MIR spectra, but peaks of weak H-B's or free O−H groups are very tiny in this region, and NIR spectroscopy is more sensitive to the weak H-B's and free O−H or N−H groups, and it is especially sensitive to the conversions of the H-B's.[56,57] As a result, the NIR spectroscopy method has been used to study H-B's in many samples, such as polymers and proteins.[53,56,57] Moreover, as novel solvents, ILs might be applied in environments with changing temperatures or high temperature conditions. Therefore, we should try to understand more thermal properties of ILs so as to make better applications. In the present work, we combine the advantages of NIR, 2D correlation spectroscopy, and PCMW methods, investigating the many interactions between water and ILs in their mixtures and ascertaining different evolution mechanisms of these interactions during the continuous heating process.

2. Experimental Section

2.1. Materials. The ionic liquid 1-butyl-3-methylimidazolium tetrafluoroborate ($bmimBF_4$) was kindly supplied by Prof. Yan at Su Chow University and was used as received (see the chemical structures in Figure 1). Deionized water was added into ionic liquid at concentrations of 15 and 2.5 mol % to make two $bmimBF_4$ samples containing different amounts of water. Each sample was stirred for 1 week before the FTIR experiments to ensure complete blending of the mixture.

2.2. Fourier Transform Infrared Spectroscopy. The FTIR spectra were recorded with a 4 cm^{-1} spectral resolution on a Nicolet Nexus 470 spectrometer equipped with a MCT detector by signal-averaging 32 scans. Glass cells (1 mm thickness), that have no absorption bands in the NIR region were used to contain the samples.

The samples of $bmimBF_4$ with water were heated from 25 to 190 °C, and variable spectra of the sample during the this process were collected every 5 °C. Baseline-correct processing was performed by OMNIC 8.0 software.

2.3. Two-Dimensional Correlation Analysis. Spectra recorded at an interval of 5 °C in heating experiments were selected in certain wavenumber ranges, and the generalized 2D correlation analysis was applied by 2D Shige software (Shigeaki Morita, Kwansei-Gakuin University, Japan). Final 2D correlation maps were drawn by Origin 8.0 software. In the 2D maps, the warm-colored (yellow-red) regions are defined as the positive correlation intensities, and the cold-colored (cyan-blue) regions are regarded as the negative correlation intensities. The slice spectra of 2D maps were also plotted by the 2D Shige software. In PCMW calculations of 2D maps, the window size is selected as $2m + 1 = 11$.

3. Results and Discussion

3.1. NIR Spectra Analysis. Figure 2a shows NIR spectra of the mixture of $bmimBF_4$ with 15 mol % water collected during heating from 25 to 190 °C. In this figure, we observe that intensities and positions of certain peaks change significantly upon heating. Because bands in NIR spectra mainly reflect vibrations of functional groups including H atoms, it is almost impossible for us to investigate the vibration of BF_4^- anions. However, through vibrations of O−H groups (in water) and C−H groups (in the imidazole ring of cation), we can accordingly find some related information of the anions, since they interact with cations and water. In Figure 2a, two absorption bands are mainly studied: the ν(O−H) overtone band (7600−6400 cm^{-1}), and the ν(C−H) overtone band (6350−5970 cm^{-1}, C−H on the imidazole ring). By analyzing these two bands, information of various interactions between water and ILs can be obtained. As a comparison, NIR spectra of $bmimBF_4$ with less water (2.5 mol %) under the same heating conditions are shown in Figure 2b. We will compare more about these two samples in further discussions.

A. ν(OH) Overtone Region. Figure 3a and b shows NIR spectra of the ν(OH) overtone region collected during heating of $bmimBF_4$ with 15 mol % water. Three obvious bands are observed, all of which decrease with time. The shapes of these three bands are very similar to those of the ν(OH) bands in the MIR region,[44] which confirms that 7600−6400 cm^{-1} is the region of ν(OH) overtones. Considering the analysis difficulties caused by the overlap of these three bands, we study their changes integratedly in the 1D NIR spectra. In Figure 3a and b, we can clearly observe that during heating, ν(OH) overtones mainly change in two aspects: (1) the band initially located at 7051 cm^{-1} gradually blue shifts to a higher wavenumber; (2) in addition to the position change, the area of ν(OH) overtones increases at the very beginning but decreases in the following heating process. As a comparison, spectra of $bmimBF_4$ with less water (2.5 mol %) under same heating conditions are shown in Figure 3c and d, in which we can see that during heating of the sample of ILs with less water, the ν(OH) overtone band also has a blue shift, and the area of this band also changes in a increase-and-decrease trend. Nevertheless, the extent of change of the position and area are both less significant as compared with those of the IL sample containing more water. We quantitatively analyze the temperature dependence of the positions and areas of the ν(OH) overtones in Figure 4 to try to understand the changes in these two samples more accurately.

Figure 4a-1 represents the temperature dependence of positions of the ν(OH) overtone peak in $bmimBF_4$ with 15 mol % water. The band is located at 7051 cm^{-1} at room temperature, and it gradually blue shifts during heating and eventually arrives at 7096 cm^{-1} at 170 °C. On the basis of previous research,[37,44,58] we know that peaks of H-B's with various strengths locate at different positions; the stronger the H-B is, the lower its wavenumber is. Therefore, the blue shift of the ν(OH) overtone peak indicates the weakening of O−H involved H-B's during heating. Although the area of the ν(OH) overtone peak in Figure 4a-2 increases during heating from room temperature to 100 °C, it decreases and finally achieves stability in the latter heating process of 110−190 °C. Thus, ν(OH) overtones show different

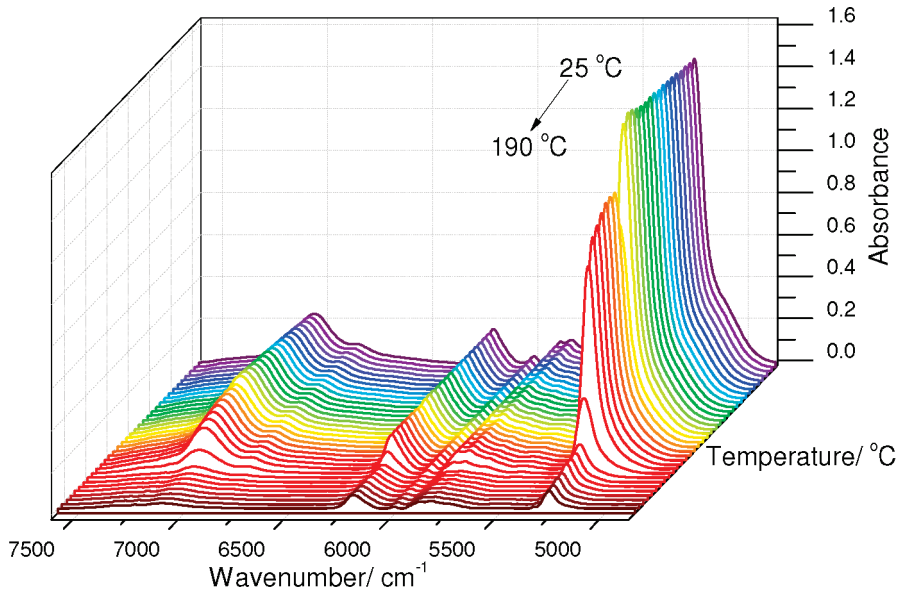

(a)

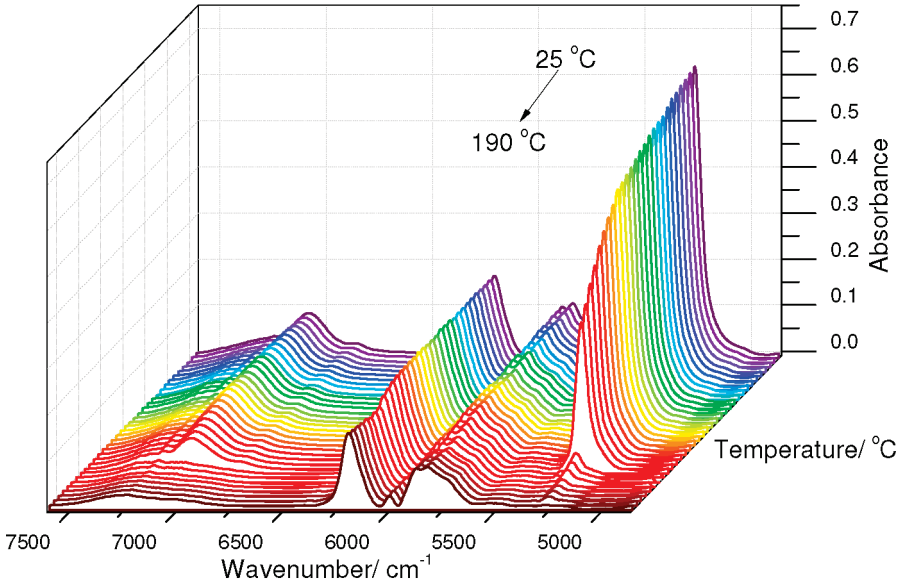

(b)

Figure 2. NIR spectra of (a) bmimBF_4 with 15 mol % water, and (b) bmimBF_4 with 2.5 mol % water collected during heating from 25 to 190 °C.

changes in different heating regions. To ascertain the critical points of these temperature regions more accurately, we performed a PCMW2D analysis of the spectra of water-containing bmimBF_4 samples during heating. The PCMW2D method correlates the external perturbations directly with changes in the peaks; therefore, it is very sensitive to the critical transition conditions of the samples.[55]

Figure 4a-3 is the asynchronous PCMW2D map in the ν(OH) overtone region of bmimBF_4 with the 15 mol % water sample. According to Morita's PCMW2D rule and our experiences,[55] we understand that temperature points in the asynchronous PCMW2D map indicate the beginning and ending temperature of peak changes. There are three temperature points in Figure 4a-3 (100, 135, and 160 °C) showing that in regions of 25−100, 105−135, 140−160, and 165−190 °C, ν(OH) overtone peaks undergo different changes. This observation is similar to the phenomenon observed in Figure 4a-2, namely the area of ν(OH) overtone peaks gradually increases during heating at 25−100 °C. In the latter region of 105−160 °C, the area gradually decreases. Within this region, the area decreases relatively slowly from 105 to 135 °C, and the area decreases faster during 140−160 °C, whereas in the final 165−190 °C region, the area achieves a stable state. Therefore, according to the behaviors of ν(OH) overtone peaks in each temperature region, we tentatively infer that:

(1) During heating at 25−100 °C, certain water-including strong H-B's dissociate into weaker H-B's or free water molecules; hence, ν(OH) overtone peaks shift to a higher wavenumber. As in the NIR region, peaks of free water or weaker H-B's appear more significant than those of the stronger H-B's, according to the dissociation of O−H involved H-B's. The area of ν(OH) overtones increases at the same time.

(2) During heating at 105−160 °C, the rest of the H-B's in the sample continue to dissociate; at the same time, a large

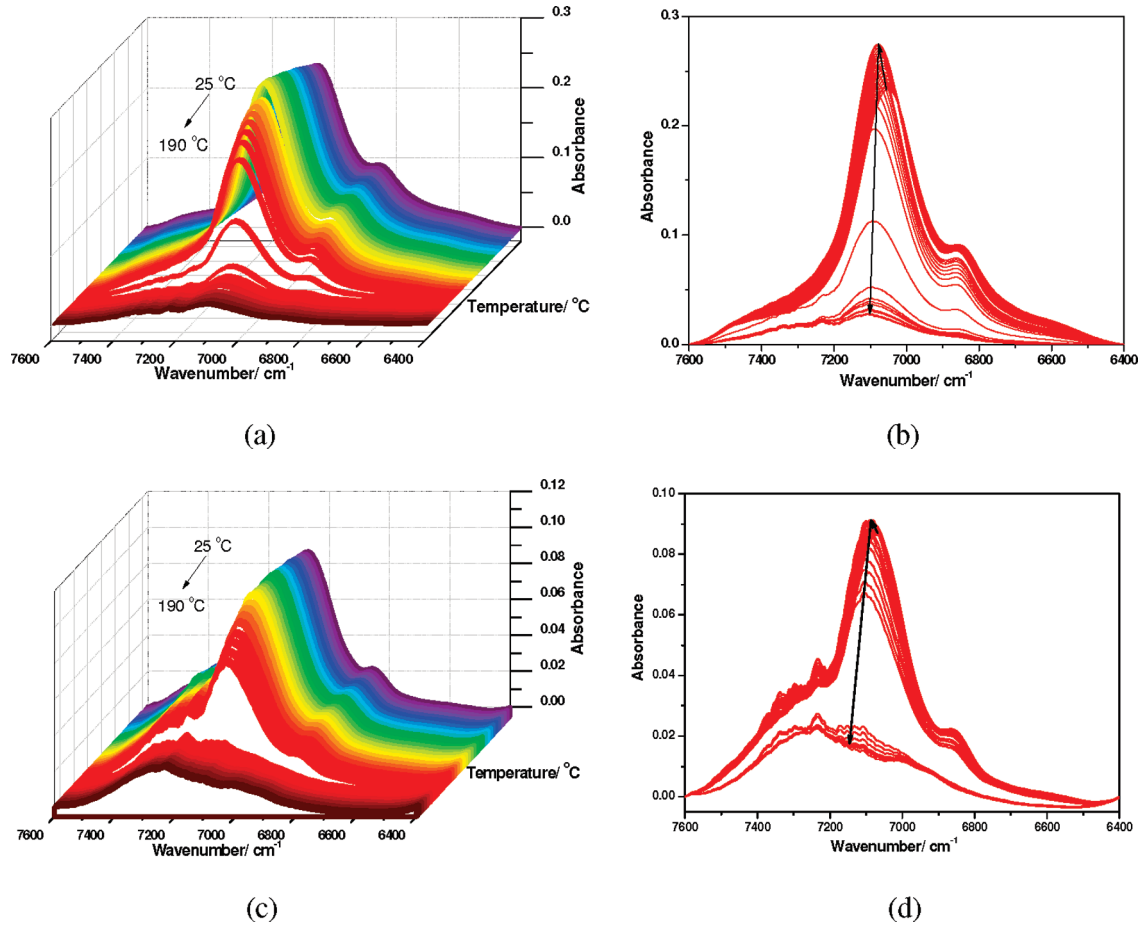

Figure 3. NIR spectra of bmimBF$_4$ with 15 mol % water in ν(OH) overtone region collected during heating from 25 to 190 °C. (a) 3D spectra, (b) 2D spectra with NIR spectra of bmimBF$_4$ with 2.5 mol % water in the ν(OH) overtone region collected during heating from 25 to 190 °C, (c) 3D spectra, and (d) 2D spectra.

number of free water molecules evaporate due to the high temperature, and therefore, the area of ν(OH) overtones greatly decreases. In this process, because the temperature is not so high (105−135 °C), the dissociation of H-B's and evaporation of water are not too fast, but within 140−160 °C, the temperature is already so high that the dissociation of H-B's and evaporation of water are much faster.

(3) In the final heating process of 165−190 °C, the dissociation of H-B's and evaporation of water is almost complete; thus, the entire system approaches stability, and the peak area shows few changes.

Although in the other bmimBF$_4$ sample with less water (2.5 mol %), we can observe from Figure 4b-1 that at room temperature, the ν(OH) overtone peak is located at 7068 cm^{-1}, this wavenumber is higher than the 7051 cm^{-1} sample of bmimBF$_4$ with more water (15 mol %), indicating that the O−H-involved H-B's in the sample containing less water are weaker than the H-B's in bmimBF$_4$ with more water. Nevertheless, we can observe in Figure 4b-1 that the ν(OH) overtone peak can also blue-shift to and stay stable at 7096 cm^{-1} at high temperature, showing that the maximum dissociation extent of O−H-involved H-B's in mixtures of bmimBF$_4$ with various amounts of water are nearly the same when the temperature is enough high. Moreover, we should note that in bmimBF$_4$ with less water (2.5 mol %), the ν(OH) overtone peak arrives at 7096 cm^{-1} at 130 °C, but in bmimBF$_4$ with more water (15 mol %), the ν(OH) overtone peak arrives at 7096 cm^{-1} at a much higher temperature (170 °C). This also shows that the more water molecules there are in bmimBF$_4$, the stronger the O−H-involved H-B's will be, and therefore, such stronger H-B's need to dissociate with more energy.

In addition, we can observe in Figure 4b-2 that the area of the ν(OH) overtone peak in the bmimBF$_4$ sample with less water (2.5 mol %) also changes less, which is likely caused by the smaller amount of water, as well. On the basis of Figure 4b-2 and b-3, we could conclude that during heating, both of dynamic behaviors and temperature regions of this area are similar to the previous sample in Figure 4a. Nevertheless, when compared with Figure 4a-3, the peak at 100 °C has a higher wavenumber in Figure 4b-3, which confirms one more time that the strength of the H-B's in bmimBF$_4$ with less water (2.5 mol %) is weaker.

B. ν(CH) Overtone Region. Figure 5a, b shows NIR spectra of the ν(CH) overtone region collected during heating of bmimBF$_4$ with 15 mol % water. Here, the C−H groups represent C−H on the imidazole ring of bmim$^+$. In these figures, we can observe that the positions of the ν(CH) overtone peaks change little in the heating process, but areas of these peaks decreases greatly at high temperature. Similarly, as a comparison, we also show the same region spectra of the bmimBF$_4$ sample with less water (2.5 mol %) in Figure 5c, d and learn that the ν(CH) overtone bands of this sample also have little shift, but the peak areas change differently, first decreasing and then increasing. To understand this situation better, we quantitatively analyze area changes of the ν(CH) overtone bands in Figure 6.

Figure 6a-1 represents the temperature dependence of the area of the ν(CH) overtone peaks in bmimBF$_4$ with 15 mol % water. According to the asynchronous PCMW2D map in Figure 6a-2, we can observe that the area of the ν(CH) overtone peaks starts

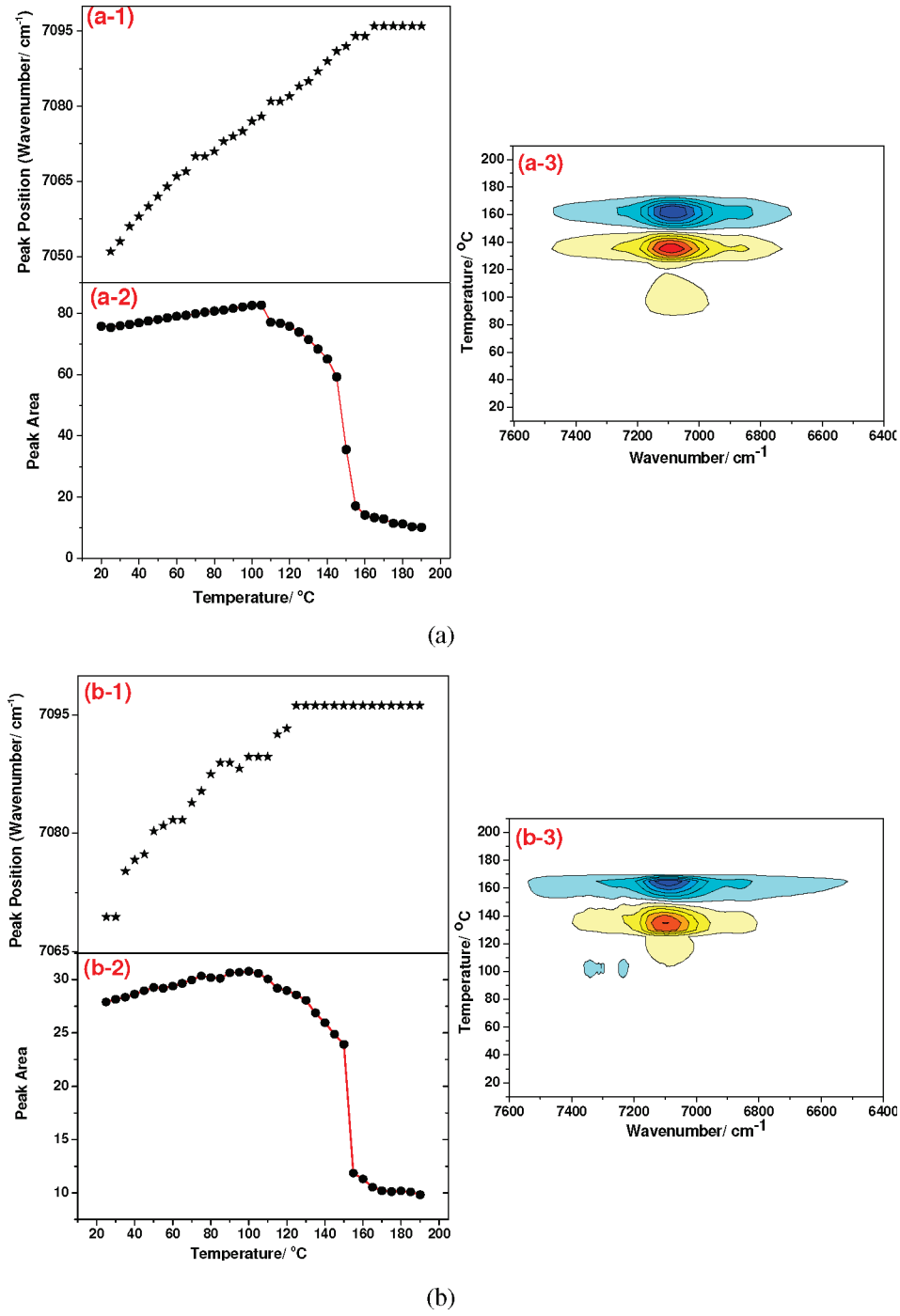

Figure 4. During heating from 25 to 190 °C, (a) in NIR spectra of $bmimBF_4$ with more water (15 mol %), the temperature dependence of position (a-1) and area (a-2) of ν(OH) overtone peak and the asynchronous PCMW2D map of the ν(OH) overtone region (a-3); (b) in NIR spectra of $bmimBF_4$ with less water (2.5 mol %), the temperature dependence of position (b-1) and area (b-2) of ν(OH) overtone peak and the asynchronous PCMW2D map of the ν(OH) overtone region (b-3).

to decrease greatly and rapidly when the temperature is higher than 135 °C and eventually achieves stability at 165 °C. For easier understanding of the dynamic mechanism of this change, we show the temperature dependence of the ν(CH) overtone peak area during heating and the time dependence of the ν(CH) peak area during the 80 °C isothermal of the $bmimBF_4$ sample with less water (2.5 mol %) in Figure 6b-1 and c, respectively.[44]

In our previous MIR spectroscopy study of interactions between $bmimBF_4$ and water during the 80 °C isothermal of the $bmimBF_4$ sample with 2.5 mol % water, we have explained clearly about the "V-shaped" area changes of the ν(CH) peaks in Figure 6c. At the very beginning of the isothermal at 80 °C, the C−H groups of the cations interact with water by H-B's; with further isothermal, water gradually evaporates and therefore induces the dissociation of H-B's between the cations and water and causes the decrease in the area of the ν(CH) peaks; later on, the cation···water H-B's completely dissociate, and lots of free cations are released. After that, these free cations would interact with free anions (released by anion···water H-B's) by new electrostatic interactions; hence, the area of the ν(CH) peaks increases again.[44]

While in the heating process of the same sample ($bmimBF_4$ with 2.5 mol % water), the area of the ν(CH) overtone peaks changes also in a "V-shape", like that shown in Figure 6b-1.

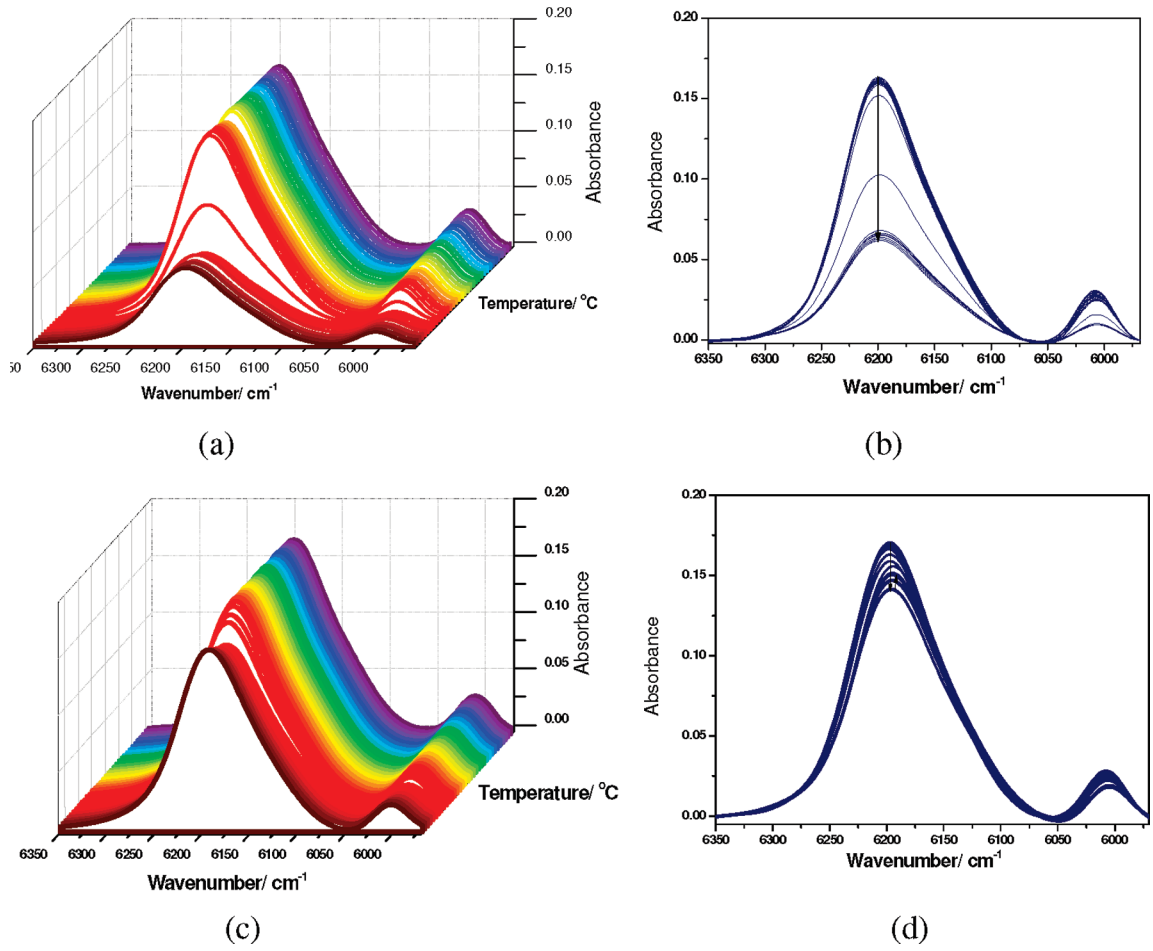

Figure 5. NIR spectra of bmimBF$_4$ with 15 mol % water in the ν(CH) overtone region collected during heating from 25 to 190 °C: (a) 3D spectra; (b) 2D spectra. NIR spectra of bmimBF$_4$ with 2.5 mol % water in ν(CH) overtone region collected during heating from 25 to 190 °C: (c) 3D spectra, (d) 2D spectra.

According to the asynchronous PCMW2D map in Figure 6b-2, we can infer that the ν(CH) overtone peak changes differently in three temperature regions: (1) 25−130 °C, this peak area changes little; (2) 135−165 °C, the area greatly decreases; and (3) 170−190 °C, the area increases again. Comparing Figure 6b-1 and Figure 6c, we can see the area of the ν(CH) overtone peaks in Figure 6b-1 cannot reverse to its initial high value in the final heating region. The possible reason is that the possibility of making contact with atoms is inversely proportional to the temperature, so when the temperature is very high, it might be harder for the cations and anions of ILs to make contact with each other, and therefore, the maximum increase of the ν(CH) peak area is smaller.

In the case of heating bmimBF$_4$ with more water (15 mol %), we can see in Figure 6a-1 that there is only the decreasing behavior of the ν(CH) overtone peaks area, but no increase in the "V-shape" appears, even with further heating. On the basis of conclusions obtained from Figure 6b and c, the decrease in the ν(CH) overtone peak indicates the dissociation of cation$\cdots$water H-B's at 135−165 °C; whereas a phenomenon of no more increasing indicates limited new cation$\cdots$anion interactions are formed during the following heating process. That is to say, due to the existence of more water molecules in the bmimBF$_4$, more and stronger H-B's would be formed between the water and cations or water and anions, and these H-B's might not be completely destroyed during heating; for these reasons, very limited numbers of free cations and anions would be released, and new interactions between them are rather finite. This can be further confirmed by the following 2D analysis.

For further understanding of the thermally induced evolutions of water−bmimBF$_4$ interactions, we investigated the ν(OH) overtone region in NIR spectra by 2D correlation analysis. 2D maps of this region reflect information of various H-B's between water and cations or water and anions in the sample. Moreover, correlation peaks in 2D maps also enable us to assign the absorption peaks in the NIR region clearly.

3.2. Two-Dimensional Correlation Analysis. The 2D correlation spectra are characterized by two independent wavenumber axes (ν_1, ν_2) and a correlation intensity axis. A pair of 2D spectra, synchronous and asynchronous maps, are generally obtained. 2D synchronous spectra are symmetric with respect to the diagonal line. Peaks appearing along the diagonal are autopeaks $\Phi(\nu_1, \nu_1)$, which are always positive. The appearance of the autopeak indicates the peak at the same wavenumber in 1D spectra changes greatly under the perturbation. Off-diagonal peaks are cross-peaks $\Phi(\nu_1, \nu_2)$, which might be positive or negative; positive cross-peaks $\Phi(\nu_1, \nu_2)$ demonstrate that both peaks ν_1 and ν_2 increase or decrease under the perturbation, whereas negative cross-peaks help to infer that the intensities of peaks ν_1 and ν_2 change in opposite directions (one increases while the other one decreases).

The 2D asynchronous spectra are asymmetric with respect to the diagonal line. Only cross-peaks would appear in asynchronous spectra, and they can be either positive or negative. With cross-peaks appearing in both synchronous and asynchronous maps, we can figure out the change orders of different peaks under the perturbation. According to Noda's rule,[45−47] if cross-peak (ν_1, ν_2) in the synchronous and asyn-

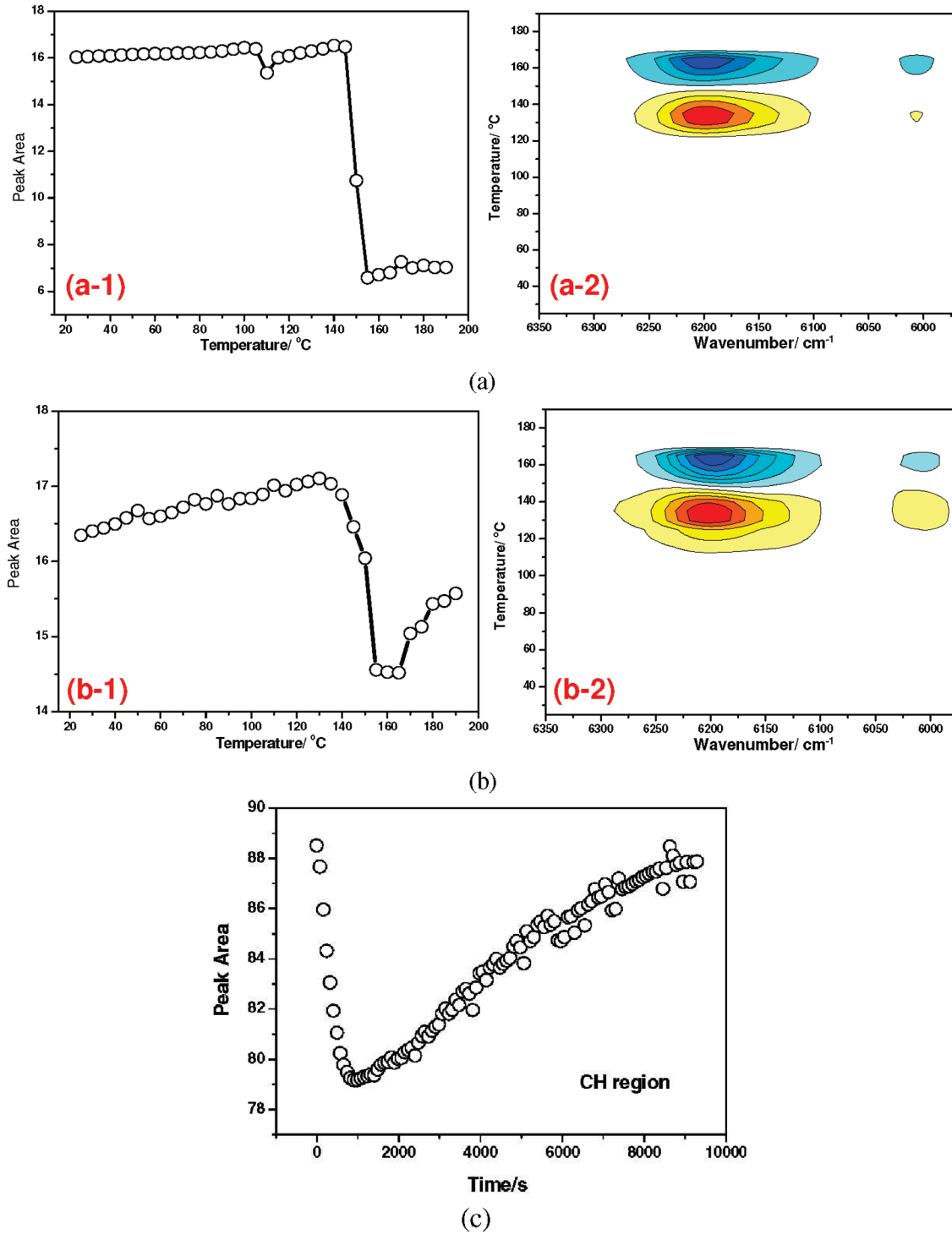

Figure 6. (a) During heating from 25 to 190 °C of $bmimBF_4$ with more water (15 mol %), the temperature dependence of the area of the ν(CH) overtone bands in NIR spectra (a-1) and the asynchronous PCMW2D map of the ν(CH) overtone region (a-2). (b) During heating from 25 to 190 °C of $bmimBF_4$ with less water (2.5 mol %), the temperature dependence of the area of the ν(CH) overtone bands in the NIR spectra (b-1) and the asynchronous PCMW2D map of the ν(CH) overtone region (b-2). (c) During isothermal at 80 °C of $bmimBF_4$ with less water (2.5 mol %), the time dependence of the area of the ν(CH) bands in MIR spectra.[44]

chronous maps has the same symbol, both positive or both negative, we can conclude that peak ν_1 varies prior to peak ν_2; but if cross-peak (ν_1, ν_2) in the synchronous and asynchronous maps has different symbols, we can conclude that peak ν_2 varies prior to peak ν_1.

Because there is little water in the $bmimBF_4$ with 2.5 mol % water mixture, the signal of the ν(O−H) region in the NIR spectra is very low, and 2D maps of this region are rough. Therefore, in this part, we only take the sample $bmimBF_4$ with more water (15 mol %) as an example to analyze the thermally induced evolutions of various microstructures by the 2D correlation method. According to the temperature regions reflected by the PCMW2D map in Figure 4a-3, we study 2D maps in three regions: (A) 25−100, (B) 105−160, and (C) 165−190 °C.

A. 2D Analysis within 25−100 °C. 2D synchronous and asynchronous maps in the ν(OH) region of $bmimBF_4$ with 15 mol % water during heating from 25 to 100 °C are depicted in

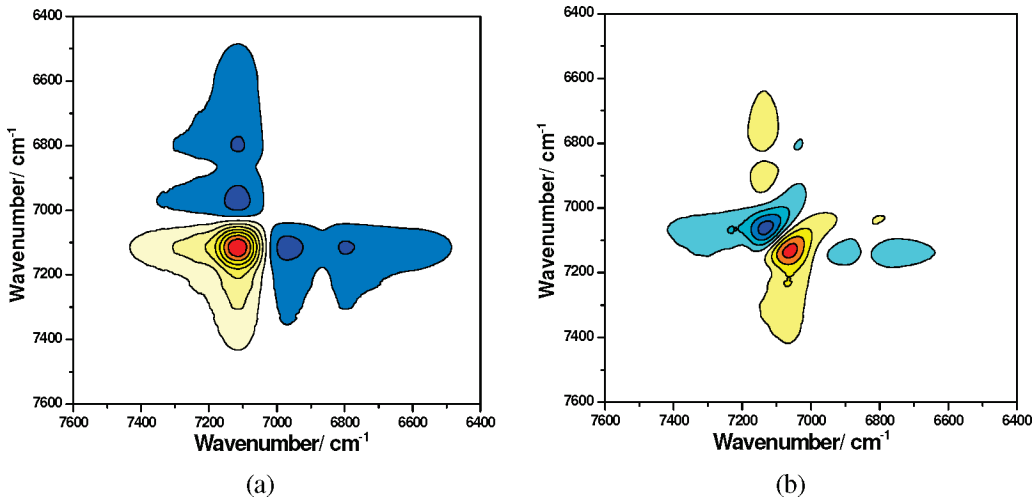

Figure 7. The synchronous (a) and asynchronous (b) maps of bmimBF_4 with 15 mol % water in the ν(O−H) overtone region during heating at 25−100 °C.

Figure 7. As shown above, changes in this temperature region mainly relate to transformations of strong H-B's to weaker H-B's or free water; thus, most correlation peaks in 2D maps would reflect vibrations of various O−H-involved H-B's or O−H groups in free water. In the synchronous map, one autopeak at 7114 cm^{-1} and two cross-peaks at (7114, 6959) and (7114, 6799) cm^{-1} are found. In the asynchronous map, three cross-peaks at (7133, 6896), (7133, 6765), and (7133, 7070) cm^{-1} are found. On the basis of previous study, we have known that there are many H-B structures in mixtures of bmimBF_4 and water. For example, BF_4^- could interact with water and form BF_4^-···water···BF_4^- or BF_4^-···cyclic water dimer···BF_4^- structures; cations can interact with water and form cation···water H-B's.[44] At the same time, H-B's between anions and water might dissociate and transform into simpler structures, such as BF_4^-···water or BF_4^-···water··· water···BF_4^-. H-B's in these microstructures have different intensities, so they should be assigned to different absorption peaks in infrared spectra. Hence, peaks in 2D maps of Figure 7 located at seven wavenumbers indicate that there are seven different O−H-involved H-B's in the current sample.

As we mentioned above, the O−H-involved H-B's and their corresponding peaks have the following relationship: the stronger the H−B is, the lower the wavenumber of the peak is.[37,44,58] Therefore, among the seven wavenumbers obtained by 2D maps, the peak with the highest wavenumber, 7133 cm^{-1}, is supposed to be the ν(OH) overtone of free water. At the same time, 7133 cm^{-1} correlates with three other peaks in the asynchronous map at (7133, 6896), (7133, 6765), and (7133, 7070) cm^{-1}, which manifests structures assigned to 6896, 6765, and 7070 cm^{-1} peaks that should be able to dissociate and release free water molecules during heating. Reading symbols of these cross-peaks in 2D maps and 2D slice maps (not shown here), we could know that:

(1) (7133, 6765) cm^{-1} is negative in the synchronous map, but positive in the asynchronous map; thus, according to Noda's rule,[45−47] we can infer 6765 > 7133 cm^{-1} (">" means "changes prior to");

(2) (7070, 6765) and (6896, 6765) cm^{-1} are negative in both synchronous and asynchronous maps, meaning 7070 > 6765 cm^{-1} and 6896 > 6765 cm^{-1}.

By linking the above orders, we can conclude 6896, 7070 > 6765 > 7133 cm^{-1}; namely, H-B structures assigned to these peaks transform in such order during heating, and 6765 cm^{-1} is a structure that can release free water directly. Exploring all possible H-B's formed by water and ILs, we find the BF_4^-···water···BF_4^- structure is able to make such transformations. During heating, it would undergo the following dissociation mode: BF_4^-···water···BF_4^- (structure I) → BF_4^-···water (structure II) → free water. There are two kinds of O−H vibrations in structure I, ν_s(OH) and ν_{as}(OH), and also two O−H vibrations in structure II, ν(bonded OH) and ν(unbonded OH). As a result, 6896 and 7070 cm^{-1} could be assigned to ν_s(OH) overtone and ν_{as}(OH) overtone in Structure I, respectively, and 6765 cm^{-1} reflects ν(bonded OH) in structure II. Here, because ν(unbonded OH) makes few contributions in this series of transformations, the 2D maps cannot reflect its position, but in the following dissociations, 2D maps clearly point it out.

In the synchronous map of Figure 7a, we note that the 7114 cm^{-1} peak forms negative cross-peaks with 6959 and 6799 cm^{-1} at the same time; namely, structures assigned to 6959 and 6799 cm^{-1} are able to transform into the structure represented by the 7114 cm^{-1} peak. Reading symbols of these two cross-peaks in 2D maps and 2D slice maps (not shown here), we could know that:

(1) (6959, 6799) cm^{-1} is positive in the synchronous map, but negative in the asynchronous map; thus, we can infer 6799 > 6959 cm^{-1}.

(2) (7114, 6959) cm^{-1} is negative in the synchronous map, but positive in the asynchronous map, meaning 6959 > 7114 cm^{-1}. Moreover, we find the cross-peak at (7133, 7114) cm^{-1} is positive in the synchronous map, but negative in the asynchronous map; thus, we can also infer 7114 > 7133 cm^{-1}.

By linking the above change orders, we can conclude 6799 > 6959 > 7114 > 7133 cm^{-1}; namely, the structures represented by the 6799, 6959, and 7114 cm^{-1} peaks gradually collapse into the next one and eventually transform into free water. Meanwhile, we note that during the transformations, peaks with low wavenumber pass onto peaks with higher wavenumbers, which also confirms our conclusions in 1D spectra: strong H-B's turn into weak H-B's during heating at 25−100 °C.

Among all H-B's formed by water and ILs, we find BF_4^-···cyclic water dimer···BF_4^- fits all the above conclusions. During heating, this H−B undergoes the following dissociations: BF_4^-···cyclic water dimer···BF_4^- (structure III) → BF_4^-··· water···water···BF_4^- (structure IV) → BF_4^-···water (structure II) → free water. There are two kinds of O−H vibrations in structure III: ν(OH···BF_4^-) and ν(double OH···OH). The

TABLE 1: Peaks and Their Assignments within ν(O−H) Overtone Region and the Dissociation Modes of Various H-B's, Calculated from 2D Maps and Slice Spectra of bmimBF_4 with 15 mol % Water during Heating at 25−190 °C

peak (cm^{-1})	assignment
7133	free water
7114	ν(unbonded OH) in $BF_4^-\cdots$water (structure II)
7033	ν(OH) in cation$\cdots$water
6959	ν(OH$\cdots$OH) in $BF_4^-\cdots$water$\cdots$water$\cdots BF_4^-$ (structure IV)
7070, 6896	ν_{as}(OH), ν_s(OH) in $BF_4^-\cdots$water$\cdots BF_4^-$ (structure I)
6799	ν(double OH$\cdots$OH) in $BF_4^-\cdots$cyclic water dimer$\cdots BF_4^-$ (structure III)
6765	ν(bonded OH) in Structure II or $\nu(BF_4^-\cdots$OH) in structure III, IV

The Dissociation Modes of H-B's during Heating

(1) $BF_4^-\cdots$water$\cdots BF_4$- → $BF_4^-\cdots$water → free water

(2) $BF_4^-\cdots$cyclic water dimer$\cdots BF_4$- → $BF_4^-\cdots$water$\cdots$water$\cdots BF_4$- → $BF_4^-\cdots$water → free water

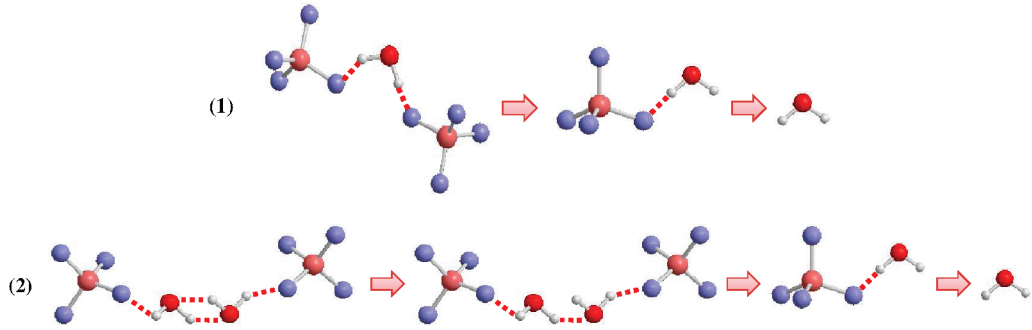

former one should be similar to the ν(bonded OH) in structure II so that 6799 cm^{-1} is assigned to ν(double OH$\cdots$OH). There are also two kinds of H-B's in structure IV: ν(OH$\cdots BF_4^-$) and ν(OH$\cdots$OH). The former vibration is similar to ν(bonded OH) in structure II, as well, so 6959 cm^{-1} is assigned to ν(OH$\cdots$OH), and 7114 cm^{-1} peak is assigned to the ν(unbonded OH) in structure II, which is able to release free water directly during heating. The position of this peak is very close to the ν(OH) of free water, which also confirms our assignments. In the current dynamic transformations, we observe ν(unbonded OH) by 2D maps, whereas in former orders, we observe only ν(bonded OH). A possible reason is that the main changes in the latter process are dissociations of O−H$\cdots$O−H, but significant changes in the former process are dissociations of $BF_4^-\cdots$O−H, and these changes affect the sensitivities of the 2D maps differently. According to the conclusions of the 2D analysis, we list the ν(OH) peaks and their assignments in Table 1.

B. 2D Analysis within 105−160 °C. 2D maps, synchronous and asynchronous, in the ν(OH) region of bmimBF_4 with 15 mol % water during heating from 105 to 160 °C are shown in Figure 8. The synchronous map shows only an autopeak at 7070 cm^{-1}, which has been assigned to the ν_{as}(OH) overtone in $BF_4^-\cdots$water$\cdots BF_4^-$ in part A. Therefore its appearance here indicates the $BF_4^-\cdots$water$\cdots BF_4^-$ structure continues to dissociate during heating within 105−160 °C.

There is a negative cross-peak (7133, 7033) cm^{-1} in the asynchronous map. According to its positive symbol in the slice synchronous map (not shown here), we can infer 7033 > 7133 cm^{-1}; namely, 7033 cm^{-1} should be assigned to a structure that releases free water directly. Because 7033 cm^{-1} has a relatively high wavenumber, this peak is supposed to represent weak H-B's. According to our previous MIR spectroscopy study on all H-B's formed by water and ILs, we can conclude that ν(OH) in cation$\cdots$water H-B's should be assigned to 7033 cm^{-1}.[44] Consequently, ON the basis of the analysis of this heating region, we understand that both H-B's between water and anions or water and cations are greatly destroyed between 105 and 160 °C; Meanwhile, according to the significant decrease of the

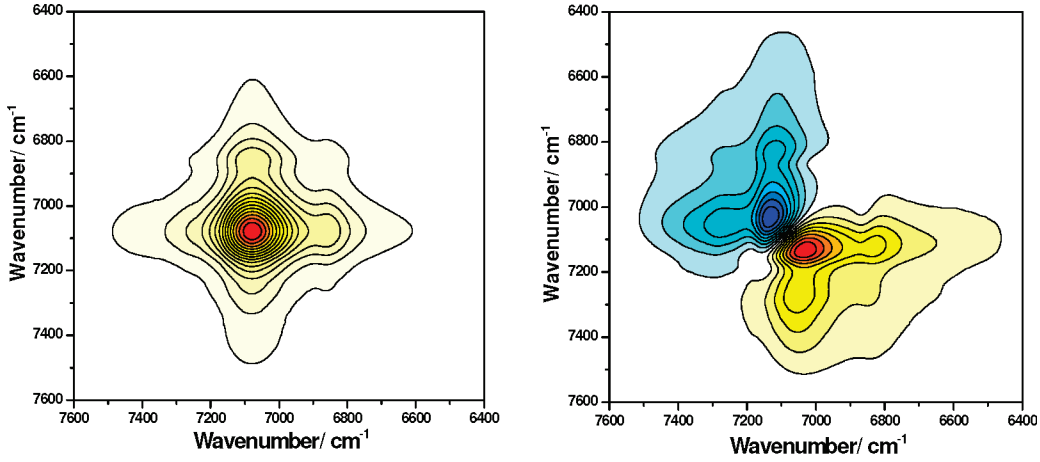

Figure 8. The synchronous (a) and asynchronous (b) maps of bmimBF_4 with 15 mol % water in the ν(O−H) overtone region during heating at 105−160 °C.

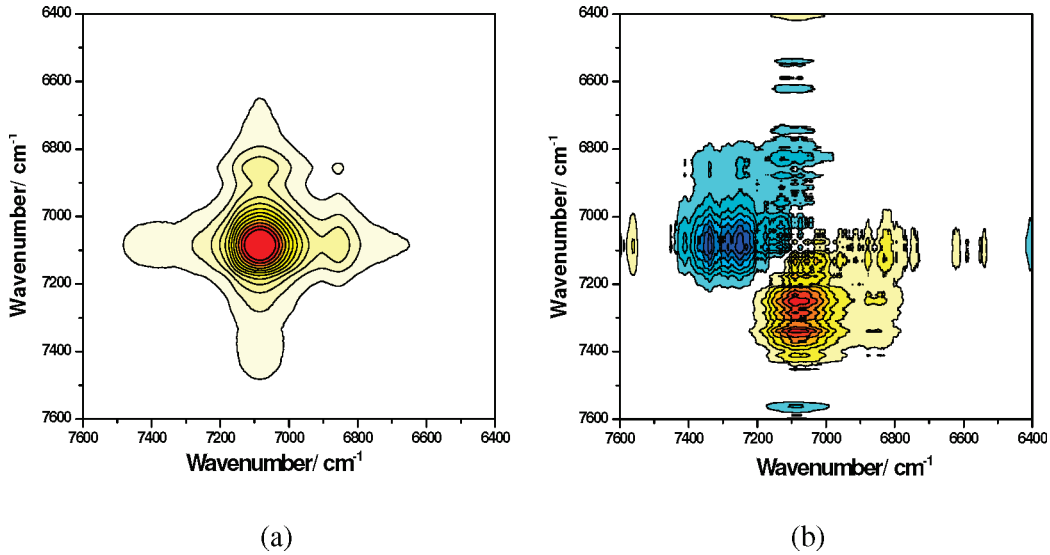

Figure 9. The synchronous (a) and asynchronous (b) maps of bmimBF_4 with 15 mol % water in the ν(O−H) overtone region during heating at 165−190 °C.

ν(OH) overtone area, the free water peak (7133 cm^{-1}) appears again, showing that a large number of free water molecules are expelled out of ILs in this heating region. We add the newly found 7033 cm^{-1} peak into Table 1, as well.

C. 2D Analysis within 165−190 °C. 2D maps, synchronous and asynchronous, in the ν(OH) region of bmimBF_4 with 15 mol % water during heating from 165 to 190 °C are depicted in Figure 9. Similar to the condition in the 105−160 °C region, the autopeak around 7070 cm^{-1} appears in the synchronous map again, which indicates that BF_4^-···water···BF_4^- still exists in the sample and continues to dissociate, even at such high temperatures. Therefore, we can infer that the BF_4^-··· water···BF_4^- structure is very stable, and this conclusion is quite consistent with our findings in a previous MIR spectroscopy study.[44]

Nevertheless, there is no clear cross peak in the asynchronous map of Figure 9 b. According to our experience, such a shape of the asynchronous map is due to the existence of water, manifesting there is a certain amount of water that remains inside the sample, even at 165−190 °C, and the existence of BF_4^-···water···BF_4^- might be one reason for such a situation. Moreover, according to the heating-induced changes of the ν(CH) peak area in Figure 6a, we remember that the area does not increase during heating at 165−190 °C, and we consider this phenomenon to be caused by incomplete dissociations of water···IL H-B's so that only limited new interactions might be formed between free cations and anions. Here, conclusions of the 2D maps in the 165−190 °C region confirm our previous deductions completely. However, the ν(OH) overtone area changes very little during 165−190 °C in Figure 4b, which indicates the number of remaining BF_4^-···water···BF_4^- is also quite limited.

Conclusions

We have investigated the thermal effect on the interaction between ionic liquids and water by NIR and 2D correlation spectroscopy methods. In the NIR spectra of bmimBF_4 mixed with more water (15 mol %), the ν(OH) overtone peak area changes differently in three heating regions. It increases at 25−100 °C, decreases at 105−160 °C, and eventually approaches stability in the final heating region of 165−190 °C. According to these three temperature regions, we study different changes of the ν(OH) overtone peaks within the three heating regions by 2D correlation analysis. According to the 2D analysis, we have observed that there are various O−H-involved hydrogen bonds in the mixture of bmimBF_4 and water (15 mol %), and assigned these microstructures clearly. In the first region, 25−100 °C, strong H-B's such as BF_4^-··· water···BF_4^-, and BF_4^-···cyclic water dimer···BF_4^- dissociate into weaker H-B's with simpler structures. In the second region, 105−160 °C, the remaining BF_4^-··· water···BF_4^- continues to dissociate, and a large amount of released free water evaporates due to high temperatures. In the final region, 165−190 °C, due to its high stability, certain BF_4^-···water···BF_4^- still exists and continues to dissociate.

Moreover, we have also investigated ν(CH) overtone peaks by comparing the isothermal process of bmimBF_4 with less water (2.5 mol %), the heating process of bmimBF_4 with less water (2.5 mol %), and the heating process of bmimBF_4 with more water (15 mol %). We have found that during the heating process of bmimBF_4 with 2.5 mol % water, although the area of the ν(CH) overtone peak also changes in a "V-shape" like the change of the ν(CH) peak area in the isothermal process of the same sample, however, in the heating process, the peak area cannot reverse back to its initial high value, even at very high temperature. We guess the possible reason for is that when the temperature is too high, the contacting possibility between cations and anions is relatively low so that fewer interactions between them can be formed, whereas in the heating process of bmimBF_4 with more water (15 mol %), the area of ν(CH) overtone peaks begins to decrease rapidly around 145 °C, but it does not increase again in the following heating process. We believe that when more water molecules exist in the ILs, more and stronger H-B's between water and ILs would be formed, and they cannot be completely destroyed, even at very high temperature. Therefore, only limited interactions would be formed between cations and anions. The 2D analysis in the heating region of 165−190 °C also confirms this; even at such a high temperature, a certain number of strong BF_4^-··· water···BF_4^- H-B's still exist.

In this study, we have understood the evolution mechanisms of interactions between water and ILs, which would be different due to the existence of various amounts of water. This observation is very helpful for practical applications of ILs in

the future. Furthermore, we have also made clear assignments of certain vibrations of ILs in the NIR region, which is also very useful for further investigations of complex systems of ILs.

Acknowledgment. We gratefully acknowledge the financial support of the National Science Foundation of China (NSFC) (Nos. 20934002, 20774022) and the National Basic Research Program of China (2009CB930000).

References and Notes

(1) Rebelo, L. P. N.; Lopes, J. N. C.; Esperanca, J. M. S. S.; Filipe, E. *J. Phys. Chem. B* **2005**, *109*, 6040.
(2) Sloutskin, E.; Lynden-Bell, R. M.; Balasubramanian, S.; Deutsch, M. *J. Chem. Phys.* **2006**, *125*, 174715.
(3) Yamaguchi, T.; Nagao, A.; Matsuoka, T.; Koda, S. *J. Chem. Phys.* **2003**, *119*, 11306.
(4) Welton, T. *Chem. Rev.* **1999**, *99*, 2071.
(5) Dupont, J.; de Souza, R. F.; Paz, S. *Chem. Rev.* **2002**, *102*, 3667.
(6) Seddon, K. R. *Nat. Mater.* **2003**, *2*, 363.
(7) Yan, F.; Texter, J. *Chem. Commun.* **2006**, 2696.
(8) Castner, E. W.; Wishart, J. F.; Shirota, H. *Acc. Chem. Res.* **2007**, *40*, 1217.
(9) Yan, F.; Texter, J. *Angew. Chem., Int. Ed.* **2007**, *46*, 2440.
(10) Dahl, K.; Sando, G. M.; Fox, D. M.; Sutto, T. E.; Owrutsky, J. C. *J. Chem. Phys.* **2005**, *123*.
(11) Shirota, H.; Funston, A. M.; Wishart, J. F.; Castner, E. W. *J. Chem. Phys.* **2005**, *122*, 184512.
(12) Urahata, S. M.; Ribeiro, M. C. C. *J. Chem. Phys.* **2005**, *122*, 024511.
(13) Hardacre, C.; Holbrey, J. D.; Nieuwenhuyzen, M.; Youngs, T. G. A. *Acc. Chem. Res.* **2007**, *40*, 1146.
(14) Borra, E. F.; Seddiki, O.; Angel, R.; Eisenstein, D.; Hickson, P.; Seddon, K. R.; Worden, S. P. *Nature* **2007**, *447*, 979.
(15) Brennecke, J. *Chem. Eng. News* **2001**, *79*, 86.
(16) Rogers, R. D.; Seddon, K. R. *Science* **2003**, *302*, 792.
(17) Garcia, B.; Lavallee, S.; Perron, G.; Michot, C.; Armand, M. *Electrochim. Acta* **2004**, *49*, 4583.
(18) Lee, S. Y.; Yong, H. H.; Lee, Y. J.; Kim, S. K.; Ahn, S. *J. Phys. Chem. B* **2005**, *109*, 13663.
(19) Matsumoto, H.; Sakaebe, H.; Tatsumi, K. *J. Power Sources* **2005**, *146*, 45.
(20) Rivera, A.; Brodin, A.; Pugachev, A.; Rossler, E. A. *J. Chem. Phys.* **2007**, *126*, 114503.
(21) Heintz, A. *J. Chem. Thermodyn.* **2005**, *37*, 525.
(22) Kelkar, M. S.; Shi, W.; Maginn, E. J. *Ind. Eng. Chem. Res.* **2008**, *47*, 9115.
(23) Gonzalez, E. J.; Gonzalez, B.; Calvar, N.; Dominguez, A. *J. Chem. Eng. Data* **2007**, *52*, 1641.
(24) Torrecilla, J. S.; Rafione, T.; Garcia, J.; Rodriguez, F. *J. Chem. Eng. Data* **2008**, *53*, 923.
(25) Rodriguez, H.; Brennecke, J. F. *J. Chem. Eng. Data* **2006**, *51*, 2145.
(26) Tong, J.; Liu, Q. S.; Xu, W. G.; Fang, D. W.; Yang, J. Z. *J. Phys. Chem. B* **2008**, *112*, 4381.
(27) Froba, A. P.; Wasserscheid, P.; Gerhard, D.; Kremer, H.; Leipertz, A. *J. Phys. Chem. B* **2007**, *111*, 12817.
(28) Ficke, L. E.; Rodriguez, H.; Brennecke, J. F. *J. Chem. Eng. Data* **2008**, *53*, 2112.
(29) Widegren, J. A.; Saurer, E. M.; Marsh, K. N.; Magee, J. W. *J. Chem. Thermodyn.* **2005**, *37*, 569.
(30) Widegren, J. A.; Laesecke, A.; Magee, J. W. *Chem. Commun.s* **2005**, 1610.
(31) Heintz, A.; Lehmann, J. K.; Wertz, C.; Jacquemin, J. *J. Chem. Eng. Data* **2005**, *50*, 956.
(32) Najdanovic-Visak, V.; Rebelo, L. P. N.; da Ponte, M. N. *Green Chem.* **2005**, *7*, 443.
(33) Lopes, J. N. A. C.; Pádua, A. A. H. *J. Phys. Chem. B* **2006**, *110*, 3330.
(34) Jiang, W.; Wang, Y. T.; Voth, G. A. *J. Phys. Chem. B* **2007**, *111*, 4812.
(35) Hanke, C. G.; Lynden-Bell, R. M. *J. Phys. Chem. B* **2003**, *107*, 10873.
(36) Cammarata, L.; Kazarian, S. G.; Salter, P. A.; Welton, T. *Phys. Chem. Chem. Phys.* **2001**, *3*, 5192.
(37) Zhang, L. Q.; Xu, Z.; Wang, Y.; Li, H. R. *J. Phys. Chem. B* **2008**, *112*, 6411.
(38) Lopez-Pastor, M.; Ayora-Canada, M. J.; Valcarcel, M.; Lendl, B. *J. Phys. Chem. B* **2006**, *110*, 10896.
(39) Huang, J. F.; Chen, P. Y.; Sun, I. W.; Wang, S. P. *Inorg. Chim. Acta* **2001**, *320*, 7.
(40) Wang, Y.; Li, H. R.; Han, S. J. *J. Phys. Chem. B* **2006**, *110*, 24646.
(41) Jain, T. K.; Varshney, M.; Maitra, A. *J. Phys. Chem.* **1989**, *93*, 7409.
(42) Gao, Y.; Li, N.; Zheng, L. Q.; Zhao, X. Y.; Zhang, J.; Cao, Q.; Zhao, M. W.; Li, Z.; Zhang, G. Y. *Chem.—Eur. J.* **2007**, *13*, 2661.
(43) Fazio, B.; Triolo, A.; Di Marco, G. *J. Raman Spectrosc.* **2008**, *39*, 233.
(44) Sun, B. J.; Jin, Q.; Tan, L. S.; Wu, P. Y.; Yan, F. *J. Phys. Chem. B* **2008**, *112*, 14251.
(45) Noda, I. *Appl. Spectrosc.* **1993**, *47*, 1329.
(46) Noda, I. *Appl. Spectrosc.* **2000**, *54*, 994.
(47) Noda, I.; Story, G. M.; Marcott, C. *Vib. Spectrosc.* **1999**, *19*, 461.
(48) Jonsson, J.; Persson, P.; Sjoberg, S.; Lovgren, L. *Appl. Geochem.* **2005**, *20*, 179.
(49) Sasic, S.; Amari, T.; Ozaki, Y. *Anal. Chem.* **2001**, *73*, 5184.
(50) Segtnan, V. H.; Sasic, S.; Isaksson, T.; Ozaki, Y. *Anal. Chem.* **2001**, *73*, 3153.
(51) Shen, Y.; Wu, P. Y. *J. Phys. Chem. B* **2003**, *107*, 4224.
(52) Sun, B. J.; Lin, Y. N.; Wu, P. Y.; Siesler, H. W. *Macromolecules* **2008**, *41*, 1512.
(53) Sun, B. J.; Lin, Y. N.; Wu, P. Y. *Appl. Spectrosc.* **2007**, *61*, 765.
(54) Wu, P. Y.; Siesler, H. W. *J. Mol. Struct.* **2000**, *521*, 37.
(55) Morita, S.; Shinzawa, H.; Noda, I.; Ozaki, Y. *Appl. Spectrosc.* **2006**, *60*, 398.
(56) Ozaki, Y.; Murayama, K.; Wang, Y. *Vib. Spectrosc.* **1999**, *20*, 127.
(57) Wu, P. Y.; Siesler, H. W. *J. Near Infrared Spectrosc.* **1999**, *7*, 65.
(58) Jeon, Y.; Sung, J.; Seo, C.; Lim, H.; Cheong, H.; Kang, M.; Moon, B.; Ouchi, Y.; Kim, D. *J. Phys. Chem. B* **2008**, *112*, 4735.

JP1041525